Contrasting Deep-water Records from the Upper Permian and Lower Triassic of South Tibet and British Columbia: Evidence for a Diachronous Mass Extinction

PAUL B. WIGNALL and ROBERT NEWTON
School of Earth Sciences, University of Leeds, Leeds LS2 9JT, UK, E-mail: wignall@earth.leeds.ac.uk

PALAIOS, 2003, V. 18, p. 153–167

Remarkably different Late Permian–Early Triassic marine records are seen in sections from the western deep-water margin of Pangea (Ursula Creek, British Columbia) and the high paleolatitude, southern margin of the Neotethyan Ocean (Selong, South Tibet). The Ursula Creek section reveals the progressive decline of seafloor oxygen values in the Changxingian Stage (loss of bioturbation, authigenic U enrichment, appearance of pyrite framboid populations), followed by the persistent development of euxinic conditions in the latest Changxingian and throughout the Early Triassic; an event that coincides with the disappearance of a siliceous sponge fauna and the loss of diverse radiolarian populations. The Selong section, which was located on a distal passive margin, records regression and erosion in the mid-Changxingian, followed by a phase of deepening that began in the late Changxingian. The boundary interval is associated with a marked diversity increase due to the appearance of equatorial taxa (foraminifera, brachiopods, and sponges), suggesting warming without extinction in marine waters at high southern paleolatitudes. Only in the late Griesbachian Stage are the diverse Permian holdovers eliminated, again at a level showing evidence for dysoxia (thinly-bedded, authigenic U-enriched, pyrite-rich limestone). Thus, the end-Permian mass extinction is seen to be diachronous by half a million years or more, with late Changxingian extinction in Panathalassa coinciding with diversity increase associated the migration of warm-water taxa into the high southerly paleolatitudes regions of Neotethys.

INTRODUCTION

Oceanographic changes during the end-Permian mass extinction have been the focus of much study in the past decade. In particular, the widespread development of oxygen-poor bottom waters in shallow-marine sections has been held as a likely cause of benthic-marine extinctions (Wignall and Hallam, 1992; Wignall and Twitchett, 1996, 2002; Twitchett and Wignall, 1996; Isozaki, 1997; Sano and Nakashima, 1997; Erwin et al., 2002; Shukla et al., 2002). The presence of organic-rich shales straddling the Permian-Triassic (P–Tr) boundary in accreted, pelagic chert sections in Japan and Thailand indicates that the anoxic event also was an oceanic phenomenon (Isozaki, 1994, 1997; Sashida et al., 2000). Potentially, a large part of the water column may have been depleted in oxygen during the P–Tr biotic crisis, but the paucity of facies data from sites recording water depths of several hundred meters (e.g., distal passive margins and continental slope locations) makes it difficult to evaluate this proposition.

In order to remedy this lack of data, redox changes have been studied from two, widely separated, deep-water P–Tr sections: the Selong section in South Tibet, dominated by condensed, pelagic limestones during most of the Early Triassic (shallower conditions occur in the P–Tr boundary beds); and the more-expanded chert and shale successions of the Ursula Creek section in British Columbia (Fig. 1). The history of P–Tr redox changes in these two regions is shown to be very different, and is compared with the equally different record of faunal turnover at these sites.

STUDY AREA AND METHODS

The section in South Tibet forms the eastern flank of Xishan, a small hill to the NW of the village of Selong (Fig. 2). The section has been the subject of intense biostratigraphic studies (e.g., Wang et al., 1989; Orchard et al., 1994), and was proposed as a candidate for the global stratotype section and point (GSSP) for the P–Tr boundary because it is one of the few sections with both abundant ammonoids and conodonts (Jin et al., 1996). The section dips steeply to the north and displays 200 m of strata. A 10 m-thick succession was measured in the center of the outcrop (section 1), from the top of the pre-Changxingian portion of the Selong Formation to the top of the Spathian Stage in the Kangshare Formation (alternatively known as the Tamba Kurkur Formation in Garzanti et al., 1998). The P–Tr boundary strata can be traced along strike for 200 m and are seen to display lateral changes. Therefore, a second section across the P–Tr boundary was logged (section 2) close to the eastern end of the outcrop. A field-portable, gamma-ray spectrometer was used to determine concentrations of Th, U, and K in section 1. Microfacies and microfossils were examined in thin section, but intense weathering has oxidized the ferrous-Fe component of the strata, thus precluding planned analyses of Fe geochemistry.

A continuous Middle Permian to Middle Triassic section is well displayed in a near-vertically dipping section on the shores of Lake Williston, British Columbia, a few kilometers west of the mouth of Ursula Creek (Fig. 2). The P–Tr transition is recorded in the cherts of the Fantasque Formation and the overlying shales of the Grayling and Toad formations. Relatively little work has been undertaken on the section, although Wang et al. (1994) recorded a negative spike in $\delta^{13}C_{org}$ and thus were able to define the location of the P–Tr boundary, confirmed here by new conodont evidence. Wignall and Twitchett (2002) reported fluctuations of Th/U ratios, based on gamma-ray spectrometer data measured on the outcrop. The microfacies and fabrics

 0883-1351/03/0018-0003/$3.00

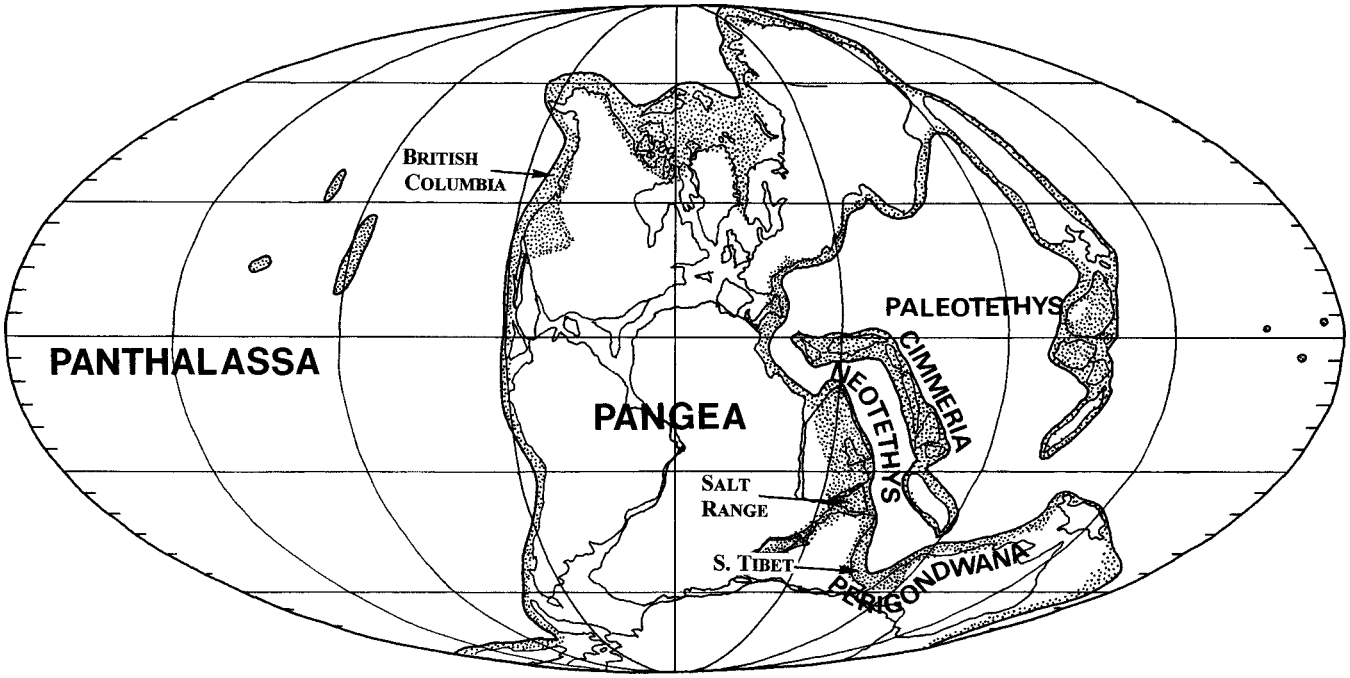

FIGURE 1—Global paleogeography during the Permian-Triassic boundary interval (based from data in Stampfli et al., 1991, Scotese and Longford, 1995, and Kobayashi, 1999).

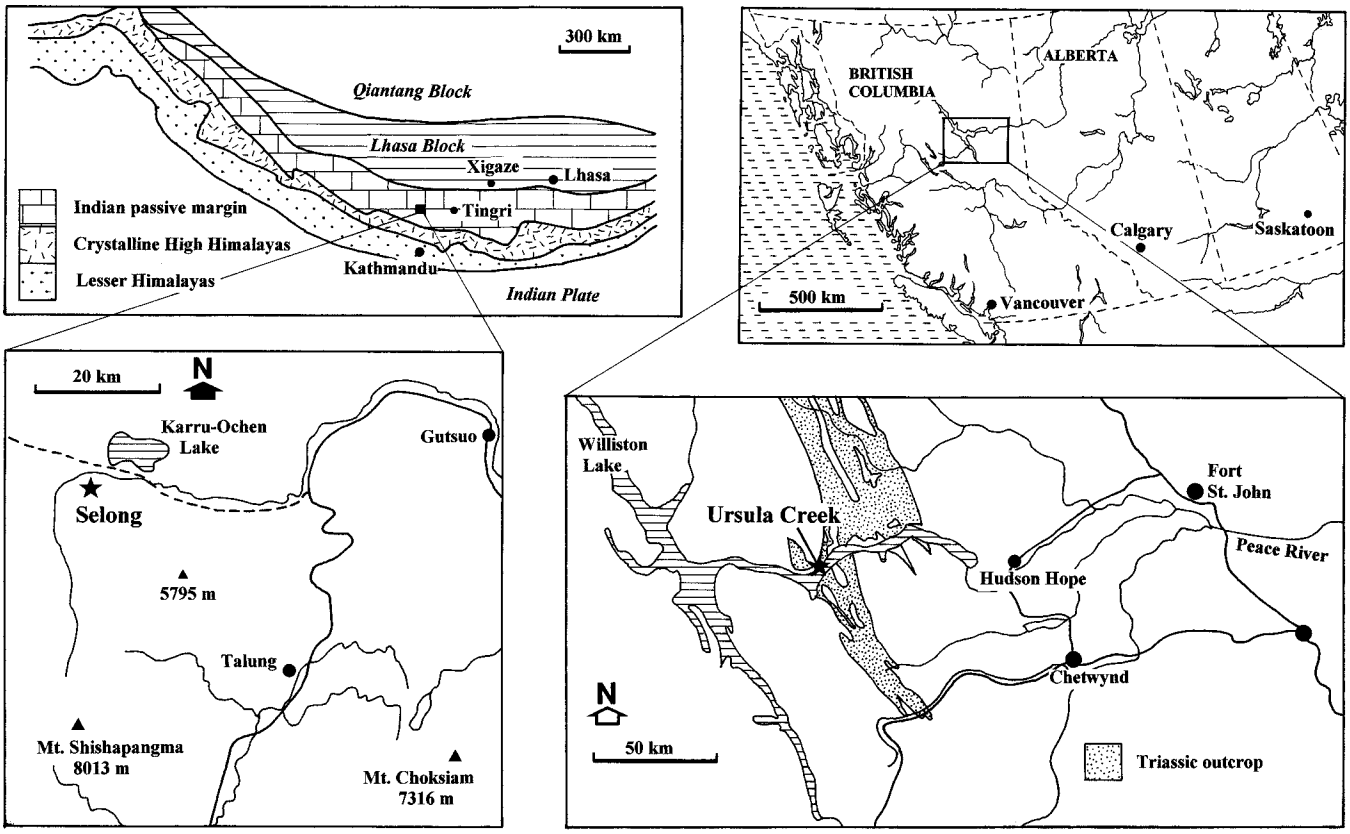

FIGURE 2—Locations of study sites in South Tibet and British Columbia.

of the section were examined in polished hand specimens, thin sections, and by SEM. Weathering has removed most original pyrite, thereby precluding Fe and S geochemical analyses, but the original texture of the pyrite (framboids, crystals) is perfectly pseudomorphed by the iron oxyhydroxide weathering products. Therefore, it was possible to assess the pyrite petrography and framboid size distributions during SEM analysis.

SELONG SECTION

Biostratigraphy

The Selong section contains both abundant conodont and ammonoid faunas that provide a fine time resolution for faunal and lithological changes within the section, although correlation with sections outside the Perigondwana region is not without controversy. The uppermost Selong Group contains only a sparse conodont assemblage, including *Mesogondolella sheni*, suggesting a Changxingian age (Mei, 1996). Conodonts become abundant in the basal beds of the Kangshare Formation, where the basal *Waagenites* Bed also contains a Changxingian conodont assemblage. The overlying *Otoceras latilobatum* Bed contains a diverse fauna dominated by *Neogondolella* spp., *Hindeodus typicalis*, and rare *H. parvus*, with *Isarcicella isarcica* appearing in the topmost centimeters (Wang et al., 1989; Orchard et al., 1994). The first appearances of *H. parvus* and *I. isarcica* define the two basalmost zones of the Triassic, and their presence at Selong indicates a complete but thin record of this key interval. The presence of *Otoceras latilobatum* with *H. parvus* may indicate an age-equivalence of the *H. parvus* Zone with the *Otoceras concavum* Zone, which is the basal Griesbachian ammonoid zone in Boreal latitudes (e.g., Yin, 1993). However, Dagys (1994) has suggested that *O. latilobatum* may be compared more closely with *O. woodwardi*, whose range is considered to coincide with the *O. boreale* Zone, the second zone of the Boreal Griesbachian (Wignall et al., 1996). Further study of Selong ammonoids is required, but for now, the conodont evidence suggests that there is a biostratigraphically complete P–Tr boundary section at Selong, with the boundary at the base of the *Otoceras* beds. The discovery of a negative carbon isotope excursion in the underlying *Waagenites* Bed provides further evidence for this age assignment because, in the best-constrained sections in both Tethyan and Boreal locations, this chemostratigraphic event occurs immediately below the *H. parvus* Zone (Wignall et al., 1996; Twitchett et al., 2001).

The age of the younger Kangshare Formation is less controversial. The presence of *Otoceras woodwardi* and *Ophiceras tibeticum*, in beds that bear their name, indicates a complete later Griesbachian, as does the increasingly rare conodont fauna (Wang et al., 1989). Garzanti et al. (1998) have identified the presence of a complete, younger Scythian record, although the boundaries of the Dienerian Stage are poorly defined due to the rarity of conodonts of this age at Selong and throughout the region.

Lithological Analysis

The topmost meters of the Selong Formation consist of coarse, crinoidal packstone with a diverse fauna, including rugose corals, bryozoans, and brachiopods (Fig. 3). The top of the unit is marked by a sharply defined bedding plane, beneath which weathering has reddened the underlying limestone to a depth of up to 20 cm. In section 1, the Selong Formation is directly overlain by additional marine limestones, but in section 2, stromatolitic masses up to 10 cm thick occur at the formational boundary (Fig. 4). In thin section, the stromatolitic laminae are seen to be intergrown with gypsum laths (Fig. 5) and to contain clasts of gray-green silty shale, a lithology that otherwise is not present in the Selong section (Fig. 6).

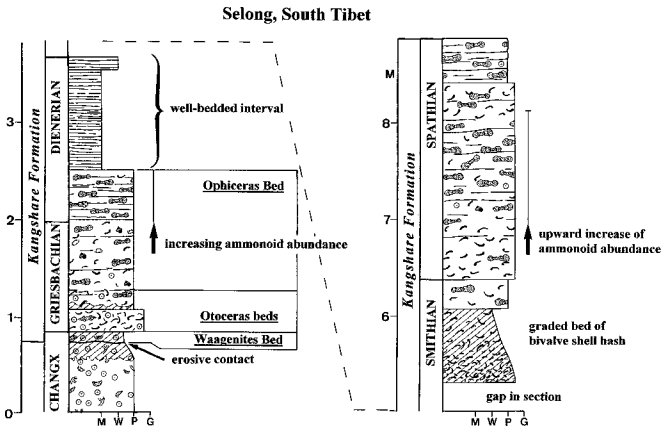

FIGURE 3—Stratigraphic section for section 1, Permian and Early Triassic boundary strata in the center of the Xishan outrop at Selong, southern Tibet (see Fig. 4 for key). Horizontal scale: M=micritic mudstone; W=wackestone; P=packstone; G=grainstone.

The basal beds of the succeeding Kangshare Formation consist of a series of frequently reddened beds, separated by sharply defined bedding planes. The basal *Waagenites* Bed, named for its brachiopod fauna, is an echinoderm wacke- to packstone in which the matrix has been replaced by rhombs of ferroan dolomite. This is overlain by the *Otoceras* beds (Fig. 4), which also are packstones with a ferroan dolomite-replaced matrix, however fragments of bivalve shells and ammonoids are somewhat more abundant than echinoderm grains at this level (Fig. 4). Pyrite cubes, 1–3 mm in width, are common in the basal centimeter of the *Otoceras* beds.

The top contact of the *Otoceras* beds marks a sharp change to well-bedded limestones. The bedding reflects the presence of well-developed, closely spaced stylolites. Ammonoid-bivalve packstones are developed in the basal meter of these Dienerian-age strata, which pass gradationally upwards into poorly fossiliferous stylonodular micrites (Fig. 3). The ammonoids are well preserved, with body chambers filled with micrite and inner whorls with large calcite crystals, whereas the thin-shelled bivalves are mostly fragmented. Replacement of the micritic matrix by rhombs of ferroan dolomite only occurs locally in these higher Kangshare beds, instead, an intergrown fabric of 10 mm-scale crystals of calcite (70%), quartz (20%), and iron oxides (10%) was seen during SEM examination. The iron oxide crystals commonly are cubic, indicating they are a weathering replacement of pyrite.

A 1.5-m gap in the section (Fig. 3) likely marks the presence of an early Smithian-age shale that is seen at this lev-

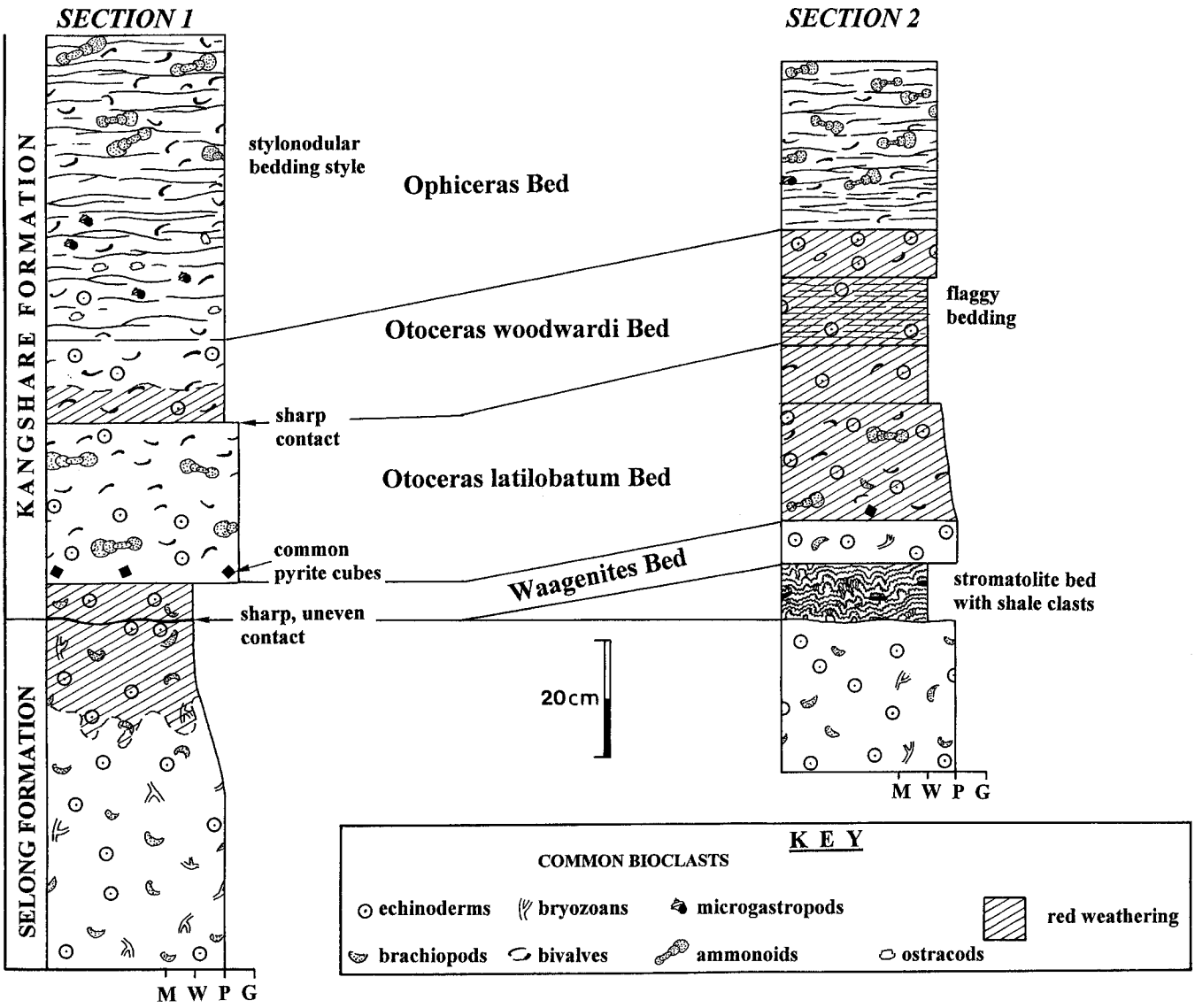

FIGURE 4—Comparison of P–Tr boundary strata in the middle (section 1) and eastern end (section 2) of the Xishan outcrops, Selong, showing local development of stromatolitic limestone at contact between the Selong and Kangshare formations. Horizontal scale: M=micritic mudstone; W=wackestone; P=packstone; G=grainstone.

el in other sections in southern Tibet (Garzanti et al., 1996). This is followed by 3 m of limestones that record Smithian–Spathian deposition. The basal 75 cm-thick bed is an orange-weathering, bivalve biomicrite that grades upwards from a packstone to a wackestone. The highly fragmented, prismatic shells derive from bivalves that were unusually large by the standards of the Kangshare Formation (Fig. 7). A hardground near the base of this bed is capped by crinkly laminae that develop locally into microstromatolites a few millimeters high.

The remainder of the Kangshare Formation at Selong consists of stylonodular, ammonoid-bivalve packstones, which is essentially the same lithology seen in the Dienerian portion of the section. Fragmentation of the fauna is low and the majority of the ammonoids lie parallel to bedding although high-angle orientations are not unusual.

Gamma-ray Spectrometry

Measured Th concentrations in the Kangshare Formation average 11 ppm, a high value compared to the average for limestone of 1.2 ppm (Faure, 1986). Th values proved equally high in the underlying Selong Formation. In contrast, the U values in the Kangshare Formation are low (1.6 ppm) compared to a limestone average of 1.9 ppm. Therefore, Th/U ratios are high throughout the section (> 3), with exception of the poorly fossiliferous interval in the Dienerian where U concentration reaches 3.4 ppm and the Th/U ratio drops to 2.8.

Faunal Analysis

The topmost beds of the Selong Formation, and the basalmost bed of the Kangshare Formation, contain an abun-

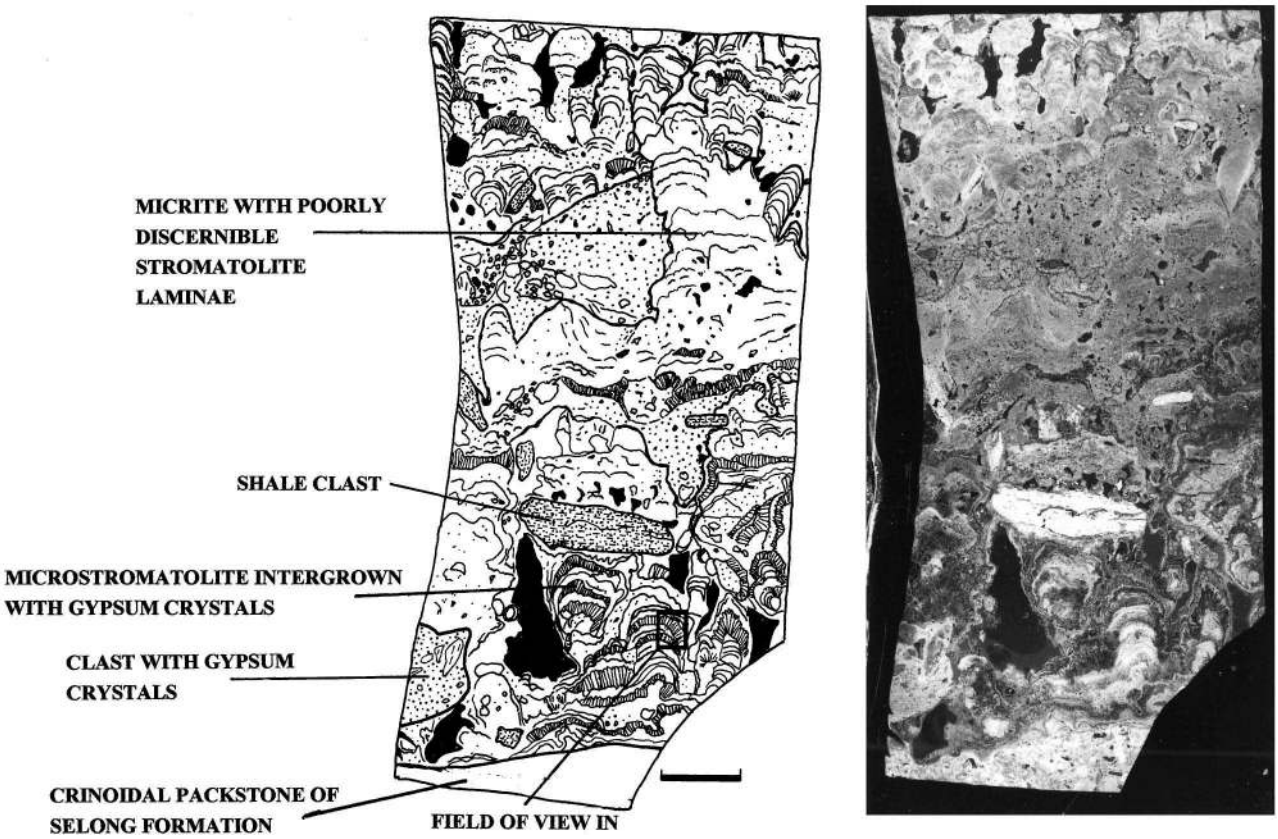

FIGURE 5—Direct print of a thin section from the stromatolite bed at section 2, Selong, with an interpretative sketch. Scale bar is 4 mm in length.

dant and diverse fauna. Only the conodonts and brachiopods have been the subjects of detailed study. *Neogondolella* species dominate the abundant conodont fauna in the *Waagenites* and *Otoceras latilobatum* beds, but the fauna becomes much rarer above this level and disappears at the end of the Griesbachian. Conodonts become diverse again in the Smithian-Spathian interval (Garzanti et al., 1998).

Brachiopod diversity increases greatly in the uppermost Selong Formation, before declining somewhat in the topmost 2.5 m of this unit (Wang et al., 1989; Shen and Jin, 1999; Shen et al., 2000). Brachiopod diversity remains moderately high in the *Waagenites* Bed, where all but two of the nine recorded species are long-ranging, Perigondwanan forms (e.g., *Spiriferella, Cleothyridinia, Krotavia, Chonetella*) that also occur in the underlying Selong Formation (Jin et al., 1996; Shen et al., 2000). However, one of the new additions is *Paracrurithyris pigmaea*, which is a common species in the equatorial sections of South China. Brachiopods also are fairly common in the *Otoceras latilobatum* Bed, although they have not been studied due to the difficulty of extraction and degree of fragmentation.

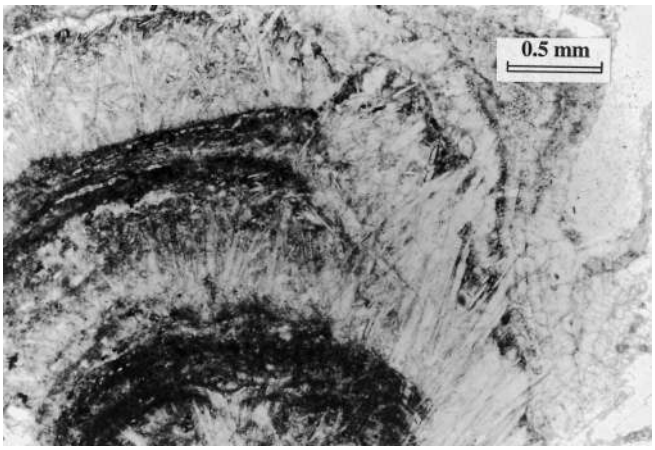

FIGURE 6—Photomicrograph showing the intimate intergrowth of gypsum laths with the stromatolitic laminae. Stromatolite bed, section 2, Selong.

Other elements of the P–Tr boundary fauna include ostracodes, rugose corals, crinoids, echinoids, bryozoans, bivalves, ammonoids, and calcareous sponges (Fig. 8). All taxa range into the base of the *Otoceras latilobatum* Bed, but the rugosans, calcareous sponges, and brachiopods, noted above, do not range into higher levels of the Triassic. The calcareous sponges, found in the both the *Waagenites* and *Otoceras latilobatum* beds, are unusual equatorial Tethyan immigrants into this Perigondwanan section (Fig. 9).

Foraminifera appear in the *Waagenites* Bed (Fig. 10) and increase in diversity up to the top of the *Otoceras woodwardi* Bed before disappearing (Fig. 8). Many of these foraminifera are typical of genera encountered in Changxingian strata from lower paleolatitude Cimmerian

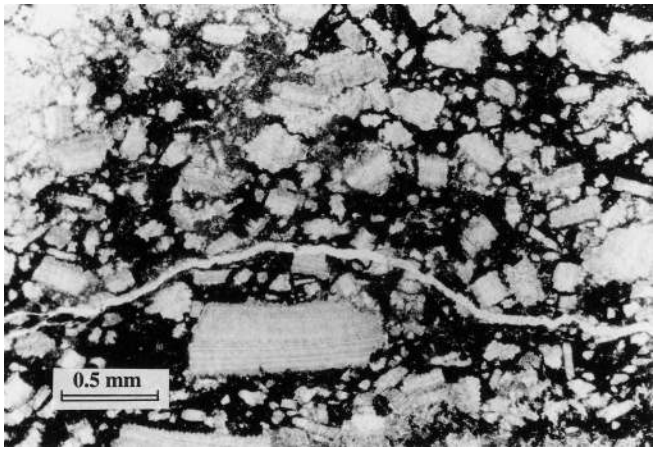

FIGURE 7—Photomicrograph of bivalve packstone from 5.4 m above the base of section 1, Selong. Blocky fragments of bivalves show both prismatic shell structure and growth banding. The ferroan dolomite matrix has been partly oxidized with the result that opaque Fe oxides are common.

terranes (e.g., *Colaniella, Agathammina, Pachyphloia, Lingulina,* and *Lasiodiscus*; Okimura et al., 1985). Two, small, rare foraminifera species, apparently congeneric with larger taxa in the *Otoceras* beds, appear at higher levels in the Kangshare Formation (Fig. 8).

The sharply defined foraminiferal extinction level at the top of the *Otoceras woodwardi* Bed marks the main level of faunal turnover in the Kangshare Formation (Fig. 8). Ophiuroids replace crinoids as the dominant echinoderm grains in the sediment, microgastropods appear and remain common throughout the formation from this level upwards, and ammonoids and thin, prismatic-shelled bivalves become dominant, although both these latter groups also are well represented in the underlying *Otoceras woodwardi* Bed. Only in the Dienerian are benthic taxa absent from the Kangshare Formation, and ammonoids become rarer at this level as well.

Depositional History

The Selong section records substantial depositional changes in the latest Permian to end-Early Triassic interval. The uppermost Selong Formation indicates shallow-marine deposition as shown by its diverse fauna. Subsequent development of a gypsiferous, stromatolite-bearing horizon records conditions typical of modern hypersaline ponds (Rouchy and Monty, 2000). This indicates a relative sea-level fall, perhaps with substantial erosion as suggested by the presence of shale clasts, prior to stromatolite growth. In more-expanded sections to the east, in the Mount Qomolongma region of Tibet and around Dolpo in NW Nepal, Wujiapingian limestones are overlain by up to 90 m of dark gray shales developed beneath dolomitic limestones of P–Tr boundary age (Bassoullet and Mouterde, 1977; Shen et al., 2001). Such shales may have been present at Selong prior to erosion and incorporation, as clasts, within the growing stromatolites. Other authors (e.g., Orchard et al., 1994; Jin et al., 1996) have recorded a 2.0–3.5 cm-thick caliche (or calcrete) bed at the top of the Selong Formation at Selong. However, the only detailed description of this bed (Jin et al., 1996), noted the presence of calcite spar and pisolite- and stromatolite-like structures, suggesting it is a thinner version of the bed described here, and not a soil horizon as suggested by the caliche epithet. Garzanti et al. (1998) have suggested that the sharp contact between the Selong and Kangshare formations could record sediment starvation during rapid transgression without the need for regression and erosional truncation, but the gypsiferous stromatolite level is clearly a very shallow-water facies that indicates regression at the top of the Selong Formation. However, we concur with Garzanti et al.'s (1998) suggestion that the subsequent depositional history recorded by the Kangshare Formation was one of rapid deepening.

Evidence for this latest Permian–earliest Triassic transgression comes from the progressive replacement of a shallow-water benthic fauna in the *Waagenites–Otoceras latilobatum* beds with a fauna dominated by more typically deep-water taxa (ammonoids, thin-shelled bivalves, neogondollellid conodonts) in the uppermost *Otoceras woodwardi* Bed and overlying strata. The failure of micritic mud to penetrate ammonoid phragmocones suggests low-energy depositional conditions with little fine-grained sediment in suspension. Only the presence of a highly fragmented bivalve fauna and a stromatolitic level in the basal Spathian bed (Fig. 3) may indicate a shallower interval of deposition within this condensed, deep-water section. Garzanti et al. (1998) compared the stylonodular, ammonoid-bivalve packstones of the post-Griesbachian Kangshare Formation to the Ammonitico Rosso facies of the Jurassic of western Tethys. This younger facies formed in distal, deep-water locations due to drowning of carbonate platforms during eustatic sea-level rise, rapid subsidence, or a combination of both. A similar origin appears appropriate for this Early Triassic development in South Tibet, with perhaps bathyal water depths being developed in the distal passive-margin locations (Garzanti, 1999).

The occurrence of oxygen-poor deposition is not manifest in the basal Triassic of Selong where the benthic fauna is diverse and abundant until the later Griesbachian. However, above this level, pyrite (now replaced by iron oxides in the intensely weathered section) becomes an abundant constituent of the sediments, suggesting oxygen-poor (dysoxic) bottom waters. However, only in the Dienerian strata, where the benthic fauna disappears and the Th/U ratio reaches a low-point, could it be argued that bottom waters become truly anoxic. The development of anoxic porewaters in the underlying sediment may explain the common occurrence of pyrite crystals in the basal part of the *Otoceras latilobatum* Bed (i.e., a case of diagenetic anoxia imposed upon a bed deposited in fully oxygenated conditions). Further evidence for the establishment of anoxic porewaters may come from the dolomitization of the matrix in pre-Dienerian strata. Dolomitization is inhibited in sulfate-bearing porewaters, but is frequent in the anoxic conditions of the sulfate-reduction zone (Burns et al., 2000).

No End-Permian Mass Extinction in South Tibet?

Permian taxa previously reported from the basalmost beds of the Triassic have been from Perigondwanan sections, but they commonly have been regarded as reworked (Bassoullet and Colchen, 1977, Garzanti et al., 1998). At Selong, Orchard et al. (1994, p. 825) noted that "The lower

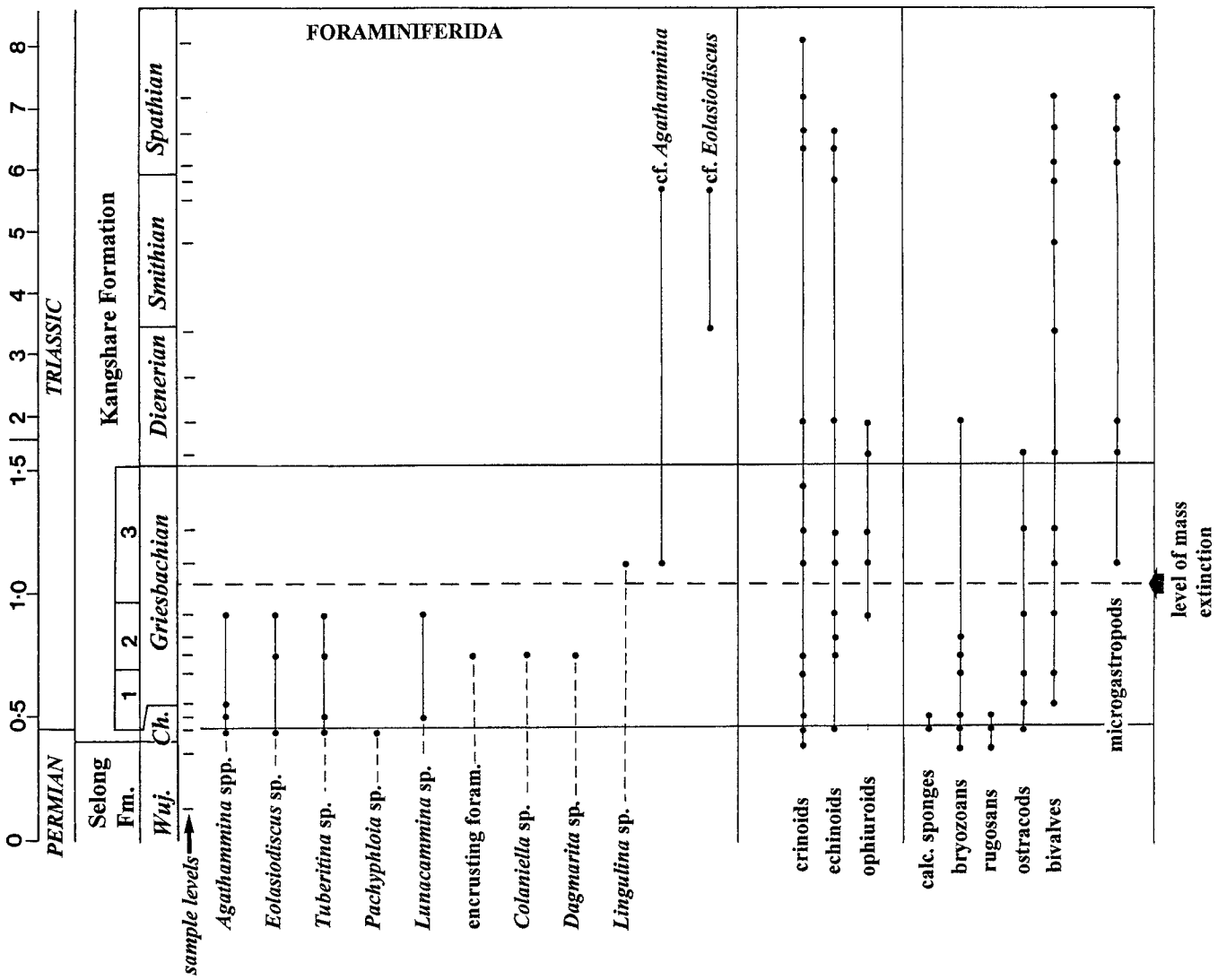

FIGURE 8—Faunal range chart of selected taxa (not including brachiopods, ammonoids, and conodonts) in the Selong section. Note scale change at 1.6 m. Beds 1, 2, and 3 are the *Otoceras latilobatum, Otoceras woodwardi,* and *Ophiceras* beds, respectively.

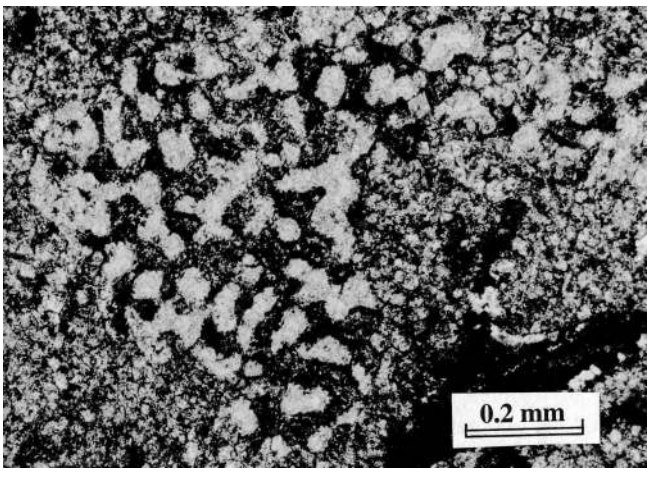

FIGURE 9—Calcareous sponge, possibly an inozoan, from the *Waagenites* Bed, Selong.

few centimeters of the *Otoceras latilobatum* bed [contain]. . . . fragments of crinoids, bryozoans and brachiopods that may be reworked." However, crinoids and other echinoderms are common throughout the Kangshare Formation (Fig. 7), not just at its base, and, although examples of abraded ossicles are common (e.g., Fig. 10D), well-preserved material, including articulated columnals, also are present throughout the formation. The foraminifera show good preservation, which together with the fact that their absence from the underlying Selong Formation (or any other unit in the Tibetan region), makes it unlikely that they have been reworked. Therefore, the fauna of the Kangshare Formation are considered to be *in situ.*

Rather than recording a mass extinction during the P–Tr transition, the Selong section shows an increase of diversity during this interval. Conodonts increase dramatically in abundance and diversity across the boundary (Orchard et al., 1994), and abundant ammonoids also appear in the base of the Triassic. Much of the benthic-diversity increase is attributable to the migration

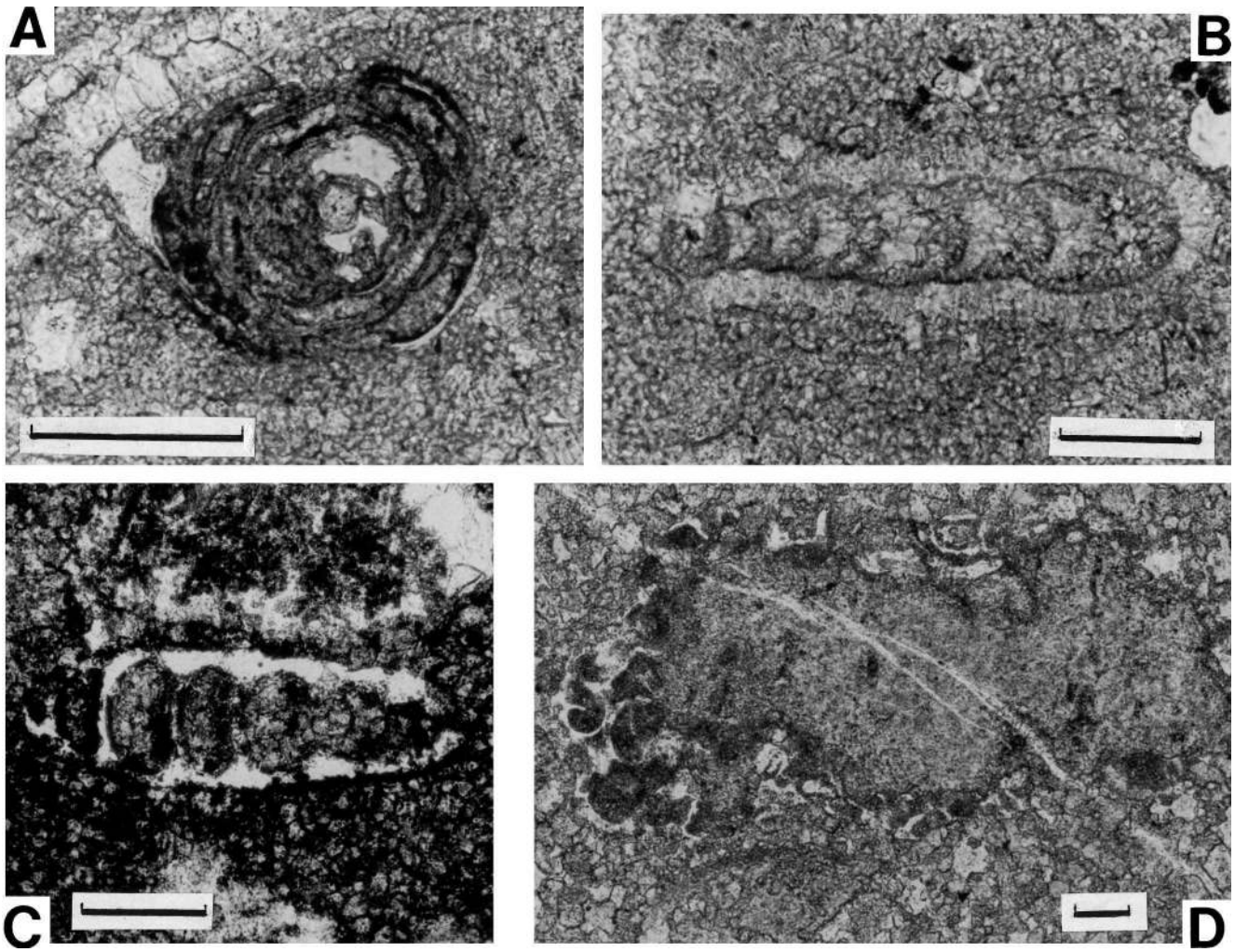

FIGURE 10—Foraminifera from the basal beds of the Kangshare Formation, Selong. (A) *Agathammina* sp. from the upper *Otoceras woodwardi* Bed. (B) *Lingulina* sp. from the basal Dienerian. (C) *Pachyphloia* sp. from the *Waagenites* Bed in a partly weathered, ferroan dolomite matrix. (D) Foraminiferan encrusting an abraded crinoid columnal. Note the micrite infill of the chambers has escaped the dolomitization seen in the surrounding matrix. Basal *Otoceras woodwardi* Bed. All scale bars 0.2 mm.

of warm-water taxa into this high-latitude location. Thus, it is intriguing to note that calcareous sponges went extinct in equatorial Tethyan locations during the late Changxingian interval (Flügel and Reinhardt, 1989; Wignall and Hallam, 1996), yet they appeared in Selong at this time and persisted into the early Griesbachian. Foraminifera show a similar pattern, but with an even greater Triassic longevity. Many of the foraminifera that appear in the basal Kangshare Beds are typical Late Permian, warm-water Tethyan taxa (e.g., *Colaniella, Dagmarita, Agathammina, Pachyphloia, Lingulina,* and *Lasiodiscus*). Their appearance at Selong marks the culmination of a southward migration of Tethyan foraminifera during the latest Permian–earliest Triassic. Thus, P–Tr boundary strata in the Salt Range, Pakistan and Kashmir, India record contemporaneous faunal changes on the Perigondwanan margin, but at a somewhat lower latitude than the Tibetan sections (50°–55°S as opposed to 55°–60°S; Fig. 1). Tethyan foraminifera, notably *Colaniella* and fusulinids, appear in Changxingian strata at these locations (Nakazawa et al., 1975; Pakistani-Japanese Research Group, 1985). *Colaniella* does not appear until the Griesbachian at Selong (Fig. 8). Equally remarkable is the appearance of *Dagmarita* at the same level, a genus otherwise known only from Late Permian, equatorial Tethyan locations (Kobayashi, 1999). *Lingulina*, another Tethyan form, is an even later arrival—it appears in considerable numbers in the late Griesbachian (Fig. 10B). All foraminifera genera at Selong disappear from equatorial locations during the late Changxingian mass extinction (Wignall and Hallam, 1996, fig. 4), yet they persist at Selong for at least half a million years (based on Bowring et al.'s, 1998 radiometric ages for this interval).

So when was the extinction event at Selong? Brachiopod diversity peaks in the upper meters of the Selong Formation before declining in abundance to modest levels that persist in the late Changxingian *Waagenites* Bed (Shen and Jin, 1999; Shen et al., 2000). However, the poorly preserved fauna of the *Otoceras latilobatum* Bed has not been studied which makes it difficult to judge the precise timing of the extinction for this group. A better appreciation of the extinction level

comes from the better-preserved foraminiferans. Peak foraminiferal diversity occurs in the basal *Otoceras woodwardi* bed (mid-Griesbachian), and the most abundant taxa (e.g., *Agathammina, Lunacammina*) range to the top of this bed (Fig. 8). The latest Griesbachian, therefore, appears to be the best candidate interval for the end-Permian mass extinction, with loss of taxa below this level attributable either to back smearing (i.e., rare taxa disappearing before the more-common taxa) or to protracted extinction within the later Griesbachian. The composition of the latest Griesbachian fauna adds more weight to the choice of this extinction interval. Microgastropods proliferated in the immediate aftermath of the end-Permian mass extinction in many Tethyan and Boreal basal Griesbachian locations (Wignall and Hallam, 1992; Twitchett et al., 2001), and they also proliferate at Selong, but in the late Griesbachian and early Dienerian. Ophiuroids are another common post-extinction fossil, and they too become common in the late Griesbachian at Selong.

URSULA CREEK SECTION

Chronostratigraphy

The cherts of the Fantasque Formation are widespread in western Canada and generally are regarded as Wordian–Capitanian age, based on their conodont fauna (Henderson, 1997). They form part of a regionally widespread, but poorly dated, chert depositional event (Murchey and Jones, 1992; Beauchamp and Baud, 2002). At Ursula Creek, limestone concretions from near the top of the Formation (Fig. 11) have yielded *Mesogondolella sheni*, an index for the late Changxingian (Henderson and Mei, 2000). This conodont also has been recovered from the topmost chert beds, indicating a Changxingian age for the upper Fantasque Formation. Thus, the Fantasque Formation at Ursula Creek either may record a prolonged phase of condensed chert deposition (from the Wordian to Changxingian stages), or may be younger than elsewhere in the region. The former alternative is preferred because a single horizon of chert deposition is seen in sections throughout western and Arctic Canada (Murchey and Jones, 1992; Beauchamp, 1994).

The Grayling Formation contains several thin dolomicrite horizons (described below). A sample of this facies from 80 cm above the base of the Formation has yielded *Hindeodus parvus*. This conodont serves to define the P–Tr boundary, which therefore must lie within the basal decimeters of the formation. This level is corroborated by the organic C-isotope data of Wang et al. (1994; Fig. 12). The C-isotope stratigraphy of P–Tr boundary sections has been determined in many sections, and those with good biostratigraphic control show a rapid decline of $\delta^{13}C$ values in the latest Changxingian, with the low point reached just beneath the conodont-defined erathem boundary (Twitchett et al., 2001). Additional negative inflexions often are developed at higher levels within the Griesbachian (Holser et al., 1991). This Ursula Creek record is particularly similar to that seen in Spitsbergen, where the low point of a $\delta^{13}C$ excursion also occurs a short distance above the level of cessation of chert deposition (Wignall et al., 1998). Additional conodont evidence indicates that the Grayling Formation spans the Griesbachian to mid-Dienerian stages, with the overlying Toad Formation ranging from the mid-Dienerian to the end of the Spathian, or even younger (Orchard and Tozer, 1997; Henderson, 1997; Moslow and Davies, 1997).

Facies Analysis

The Fantasque Formation consists primarily of radiolarian and spiculitic chert, with minor dark-gray shale interbeds. Decimeter-thick beds of chert separated by centimeter-thick partings of shale are typical, although thicker beds of chert and shale also are present (Fig. 11). The contact between the Fantasque and Grayling Formations is sharp and marks the loss of cherts, which are replaced by dark-gray shales displaying papery fissility and, at higher levels in the formation, less-fissile shaly mudstones. Interbedded with the shales are distinctive, laminated, orange-brown weathering beds ranging from 1–35 cm thick. Henderson (1997) suggested these beds were siltstones that marked the culmination of small-scale coarsening-upwards units, but thin-section and SEM analyses reveal them to be comprised of a mosaic of small dolomite rhombs and organic-rich laminae. Two heavily recrystallised filamentous limestones occur towards the top of the formation.

The Toad Formation in British Columbia and Alberta is reported to consist of calcareous siltstones, silty limestones, and minor silty dolomites, with turbiditic sandstones developed in the eastern-most outcrops (Moslow and Davies, 1997). At Ursula Creek, its most westerly outcrop, the Toad Formation consists of dark-gray to black siliceous shales interbedded with calcareous cherts containing large carbonate concretions. The latter lithology resembles a laminated siltstone on outcrop, but petrographic examination reveals the majority of the grains to be spheres of calcite that probably are replaced radiolaria, with only minor silt-grade quartz grains (Fig. 13). The matrix consists of intimately intergrown calcite and silica in equal proportions. Therefore, the Toad Formation siltstones more correctly are termed calcareous radiolarites.

Three distinct fabrics are present in the Ursula Creek section, with each having its own, distinctive pyrite petrography:

(A) Bioturbated fabric occurs in the lower part of the Fantasque Formation. Burrow margins are diffuse, suggesting a soft substrate, although burrows resembling *Diplocraterion, Teichichnus,* and *Planolites* can be discerned. Bioturbated fabric is devoid of pyrite.

(B) Microburrowed fabric occurs in the upper Fantasque Formation. The burrows generally are less than 2 mm in diameter, horizontal to bedding, and have not disturbed the thin bedding/lamination of the sediment. Pyrite is moderately common in this fabric and occurs as crystals, amorphous void-filling forms, and, rarely, as framboids that show a broad size range, with mean framboid diameter typically greater than 8 μm (Fig. 14a).

(C) Laminated fabric occurs throughout the Grayling and Toad Formations and at discrete levels in the Fantasque Formation, with the lowest development, a thin bed of shale, occurring 10 m below the top of the formation (Fig. 11). Pyrite is common and occurs mostly in framboidal form, with 80–90% of the framboids less than 8 μm in diameter (Fig. 14b).

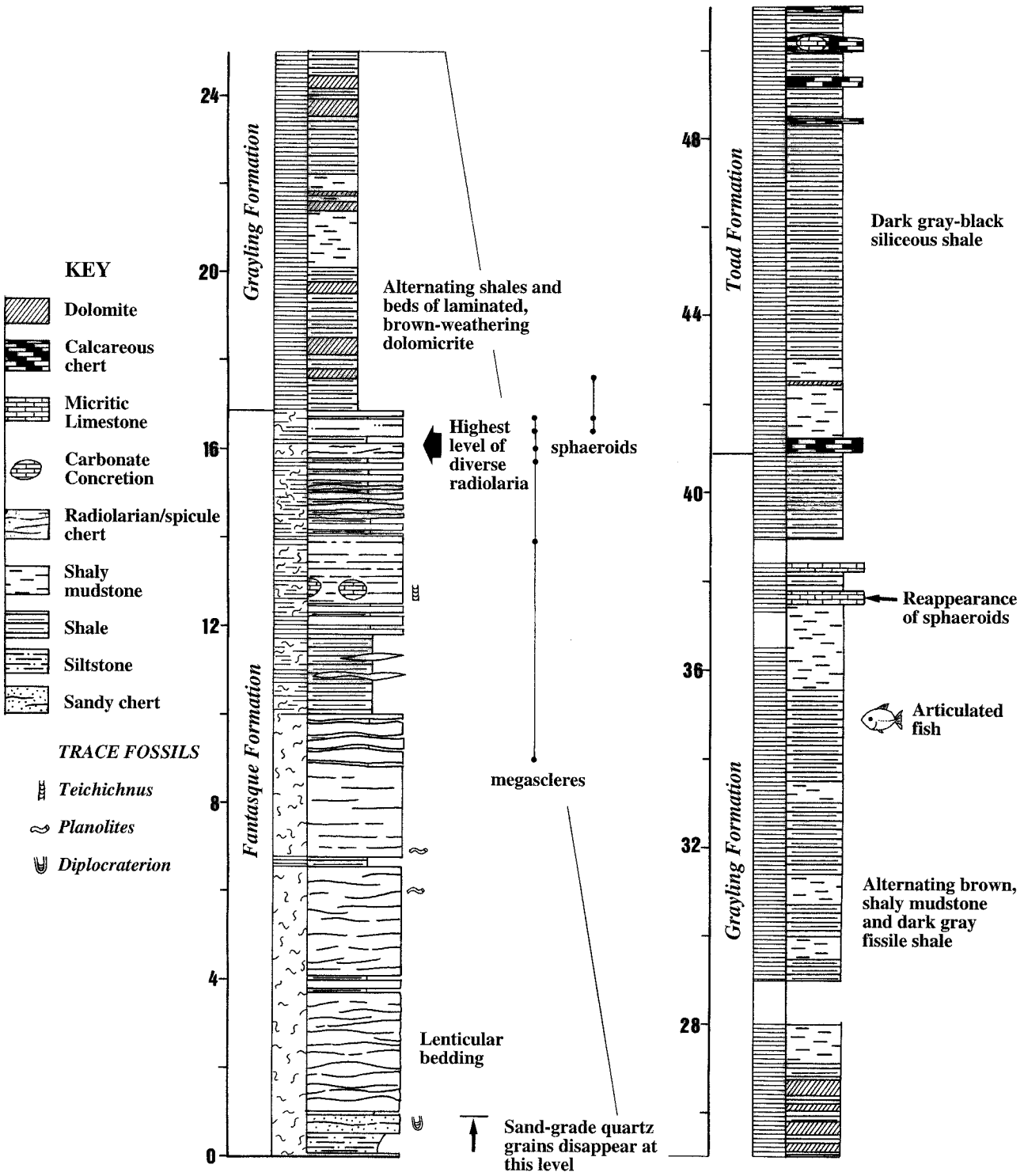

FIGURE 11—Stratigraphic section of Upper Permian–Lower Triassic strata, Ursula Creek, British Columbia. See Figure 12 for sediment fabric key. The Lower Triassic strata consist of finely laminated, anoxic facies, thin examples of which also occur in the Upper Permian.

Gamma-ray Spectrometry

Wignall and Twitchett (2002) presented data for U and Th fluctuations in the Ursula Creek section, so only the salient features are highlighted here. Both Th and U concentrations are low (less than 6 ppm and 2 ppm respectively) in the bioturbated and microburrowed facies of the Ursula Creek Formation, but both increase in the topmost meter of the formation and remain high throughout the remainder of the section (Th $>$ 8 ppm, U $>$ 5 ppm). The Th/U ratio within the laminated shale facies is consistently between 1 and 2.5.

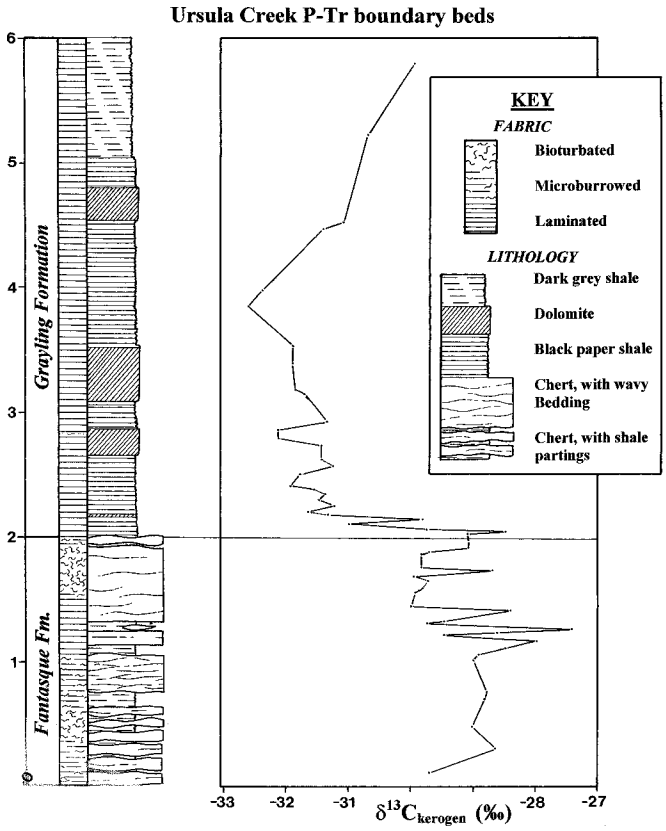

FIGURE 12—Lithological and $\delta^{13}C_{org}$ changes in the vicinity of the P–Tr boundary at Ursula Creek. Carbon isotope data from Wang et al., 1994.

Faunal Analysis

Radiolaria are abundant in cherts of the Fantasque Formation, with the most-diverse assemblages (as determined in thin section) occurring towards the top of the formation (Fig. 11), where the assemblage includes representatives of the Entactinaria and Grandetorturiidae (Fig. 15). Only indeterminate, small chalcedony-filled spheres (radiolaria?) are present in the top 75 cm of the Fantasque Formation, a few of which range up into the laminated dolomite bed 75 cm above the base of the Grayling Formation. As noted above, small, simple radiolaria (spheroids) reappear in the Toad Formation.

Well-preserved monaxon spicules of siliceous sponges are common in the uppermost meters of the Fantasque Formation, and megascleres up to 1 cm in length are common locally. In detail, the sponge fauna is common in the bioturbated beds and absent from the laminated strata. The Lower Triassic formations of Ursula Creek lack macrofossils, except for the rare presence of well-preserved fish (cf. *Bobastraenia*) in the upper Grayling Formation (Fig. 11).

Oxygenation History at Ursula Creek

The Ursula Creek record indicates a progressive deterioration of oxygen levels during the Late Permian. The bioturbated, pyrite-free cherts of the Fantasque Formation record well-oxygenated seafloor conditions that occur at several levels up to the latest Changxingian (Fig. 11). The microburrowed facies records more-dysoxic conditions in which only a small, shallow-burrowing mobile infauna was present—a common feature of dysaerobic facies (Wignall, 1994). The relatively large framboid populations also are characteristic of dysaerobic sediments in which framboids grow in anoxic conditions within the sediment. Thus, their size was controlled by the local availability of reactants (Wilkin et al., 1996).

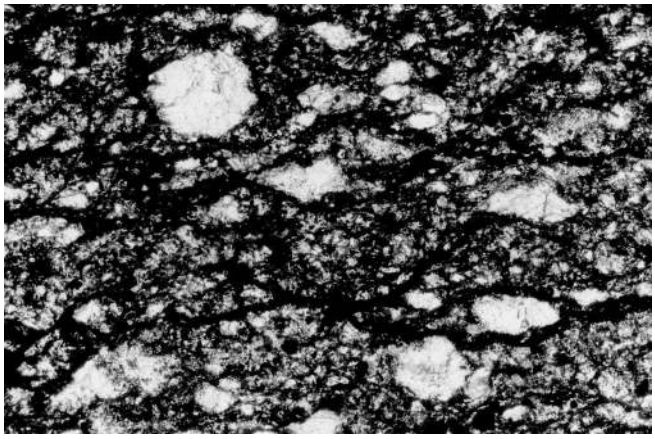

FIGURE 13—Photomicrogrph of a calcareous chert for the Toad Formation, Ursula Creek, showing numerous calcite-filled spheres, or spheroids, interpreted to be replaced radiolaria. The largest sphaeroid is 0.25 mm in diameter.

True seafloor anoxia is indicated by the finely laminated, benthos-free strata that characterizes all of the Grayling and Toad Formations, and several thin intervals of the Fantasque Formation. The associated small pyrite-framboid populations are characteristic of euxinic waters where framboids form at the redox boundary within the water column, but sink rapidly before they grow to larger sizes. In modern euxinic environments, such as the Black Sea, framboid diameter rarely exceeds 6 μm (Wilkin et al., 1997), but in the Ursula Creek laminated strata, a small proportion of framboids are larger than this threshold val-

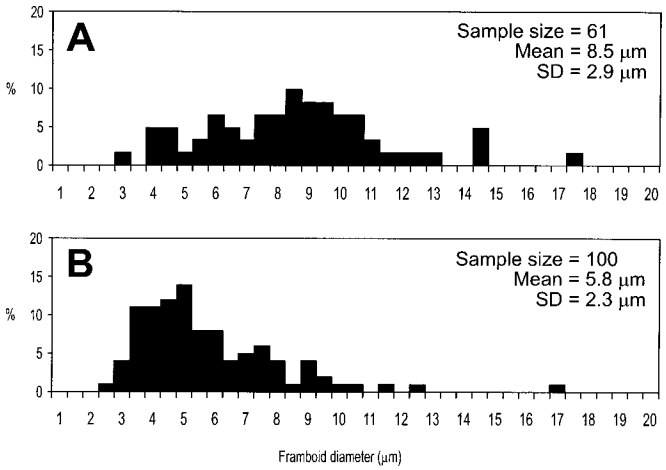

FIGURE 14—Pyrite framboid size distributions from the Ursula Creek section from (A) the topmost chert of the Fantasque Formation; and (B) a laminated dolomite from 1.3 m above the base of the Grayling Formation.

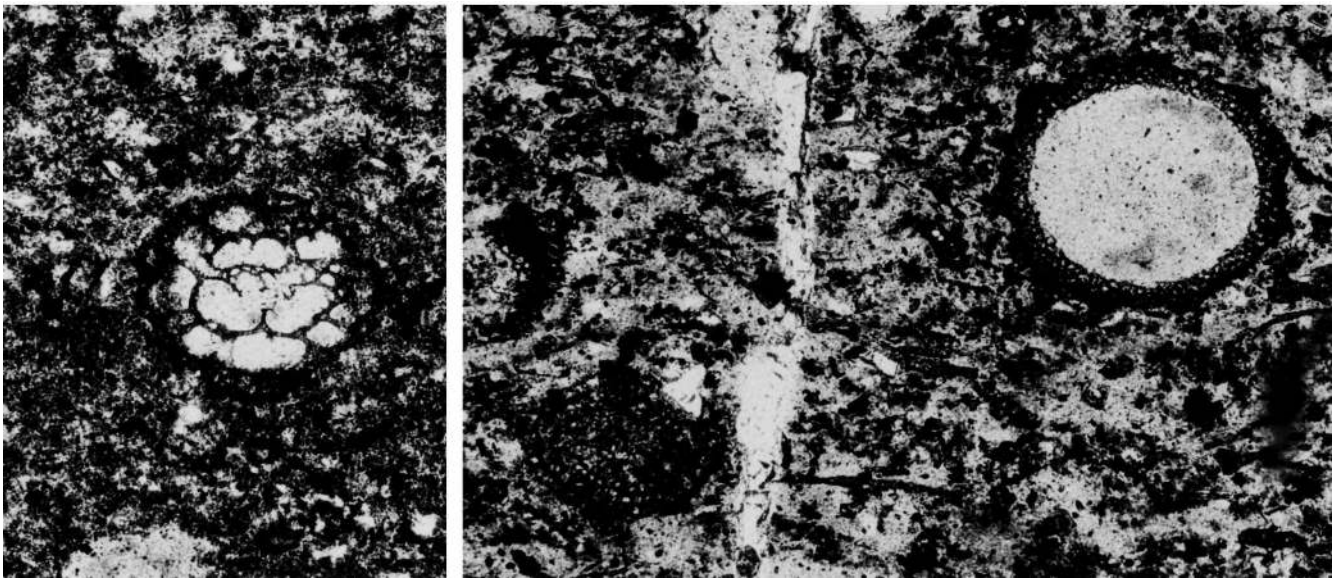

FIGURE 15—Photomicrographs of radiolaria from the Fantasque Formation (sample 85 cm from the top of the Formation) showing representatives of the Grandetorturiidae (on the left), the Entactiniidae, probably *Copicyntra*, in the middle, and an indeterminate spumellarian on the right. All to the same scale; the spumellarian is 0.4 mm in diameter.

ue. Such size-frequency distributions are characteristic of euxinic conditions punctuated by brief seafloor oxygenation events that cause the redox boundary to shift from the water column to the sediment where larger framboids are able to grow (Wignall and Newton, 1998). Evidence for brief reoxygenation events in many shelfal black shales also comes from the presence of an opportunistic benthic fauna. This is not seen in the Ursula Creek strata, perhaps because the oxygenation events were too brief or the dispersal distance was too great.

The oxygenation history interpreted from the sediment fabric and pyrite petrography also is supported independently by gamma-ray spectrometry data. The increase of both Th and U contents above the Fantasque Formation reflects both loss of biogenic silica and increased detrital components in the Lower Triassic strata, including U- and Th-bearing heavy minerals. However, the relatively greater enrichment of U (Th/U ratios decline below 3) records an additional source of U via authigenic precipitation from anoxic bottom waters (Myers and Wignall, 1987).

Extinction Record at Ursula Creek

Oxygen decline at Ursula Creek is seen first in the middle of the Fantasque Formation, and occurs in a stepwise manner before the transition to persistent anoxia in the latest Changxingian (i.e., at the base of the Grayling Formation). This level coincides with the disappearance of the abundant siliceous sponge fauna, while the last diverse radiolarian assemblage disappears somewhat below this level, with low-diversity populations of spheroids occurring abundantly in the topmost beds of the Fantasque Formation. The spheroids persist into the basal Grayling Formation. Thus, extinctions at Ursula Creek are related closely to the onset of a prolonged phase of anoxic deposition. If the radiolaria lived deep in the water column, then they too could have been affected by the anoxicity, with the simplest forms living highest in the water column being the last to go extinct, if it is assumed that the anoxia developed from the bottom up as indicated by the pyrite-framboid data. A drastic decline in nutrient availability associated with a decline in water-column circulation also could have been an important factor in radiolarian extinction (Hallam and Wignall, 1997, p. 140–141).

The harsh, anoxic depositional conditions recorded at Ursula Creek persisted throughout the Early Triassic, with the appearance of radiolaria in the late Dienerian (basal Toad Formation) being the first (and only) evidence of recovery in this interval, although the taxonomic affinities of the poorly preserved spheres is enigmatic. Elsewhere in Early Triassic pelagic facies, the initial recovery of radiolarians also is recorded by development of indeterminate spheroids in the Smithian, before more diverse and identifiable forms appear in the Spathian (Yao and Kuwahara, 1997).

DISCUSSION

Both the Tibetan and British Columbian sections record Permian to Triassic conditions on an ocean-facing continental margin (Fig. 1). Deposition was probably in water hundreds of meters deep, as suggested by the widespread development of pelagic facies (ammonitico rosso-type limestones or radiolarites) that lack evidence for current or wave activity. In the Selong section, such conditions are developed only in the Early Triassic following shallow-marine Late Permian deposition. This probably reflects the development of a distal passive margin following a regional rifting event in the mid-Permian (Stampfli et al., 1991; Liu and Einsele, 1994; Garzanti et al., 1998). Despite the similarity of their depositional settings, the Selong and Ursula Creek sections reveal a remarkably different record of the end-Permian environmental crisis.

The faunal trends in the British Columbia section com-

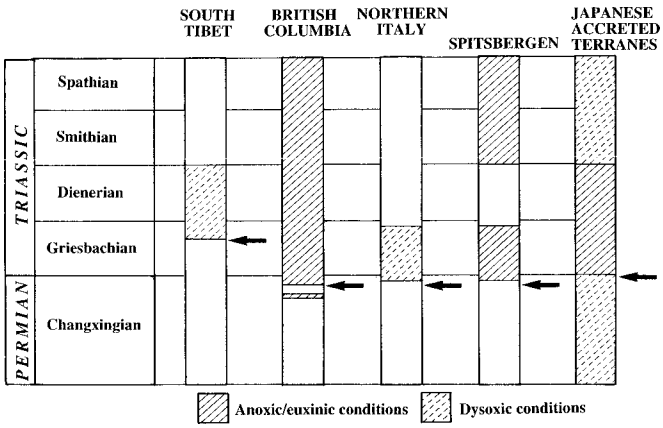

FIGURE 16—Summary and comparison of Permian-Triassic oxygenation histories and extinction levels in South Tibet and British Columbia (data presented here) with evidence from northern Italy (Wignall and Hallam, 1992; Wignall and Twitchett, 2002), Spitsbergen (Wignall et al., 1998), and Japanese accreted terranes (Isozaki, 1994, 1997). Arrows mark the extinction level.

pare closely with those from shallower-water facies in numerous locations (e.g., northern Italy and Spitsbergen), where the disappearance of late Changxingian benthic forms coincides closely with the development of oxygen-poor deposition (Wignall and Hallam, 1992; Wignall et al., 1998; Fig. 16). The radiolarian populations also were thriving up to this point in British Columbia, and they too underwent a dramatic extinction, although simple forms persisted into the earliest Griesbachian. The subsequent depositional history (persistent anoxia throughout the Early Triassic) contrasts with that seen in Tethyan sections, where the anoxic event is restricted to the Griesbachian Stage (Wignall and Twitchett, 2002). However, it compares closely with the Panthalassa Ocean records of Japan, which reveal a superanoxic event of similar duration (Isozaki, 1994, 1997; Fig. 16), and with the Californian record where anoxic deposition persisted into the later Early Triassic (Woods et al., 1999; Woods and Bottjer, 2000).

Paradoxically, the South Tibet section records an increase of benthic diversity at the time of the end-Permian mass extinction, due to the appearance of equatorial Tethyan forms (foraminifera, brachiopods, calcareous sponges). Only in the late Griesbachian do these taxa disappear at a level that also records a decline of benthic oxygen levels, although only to dysoxic rather than truly anoxic levels. This distinctly out-of-phase history appears to be characteristic of the entire Perigondwana region. Thus, Wignall and Hallam (1993) have argued that anoxia developed only in the Salt Range sections of Pakistan in the latest Griesbachian. The persistence of diverse Permian holdover taxa also appears to be a regional event. Permian-type brachiopods and bryozoans have been reported from *Otoceras concavum* Zone limestones from Nepal (Bassoullet and Colchen, 1977; Waterhouse, 1977), although they usually are considered reworked. This is unlikely, at least for the Tibetan taxa, because they belong to forms not seen in the underlying Permian.

The differing oxygenation histories and extinction timings of Tibet and British Columbia may record distinct circulation regimes. Rapid global warming is envisaged to have occurred in the latest Permian (Retallack, 1999), as evinced by the appearance of equatorial Tethyan taxa in the high paleolatitudes of South Tibet. This is interpreted to have resulted in a reduced equator-to-pole temperature gradient, which caused a decline in oceanic circulation (Wignall and Twitchett, 1996). Recent computer modelling confirms this interpretation, with oceanic circulation in a Pangea-configuration world being particularly susceptible to changes of productivity levels and temperature in high-latitude surface waters (Hotinski et al., 2001). Such modeling treats the Panthalassa and Tethyan oceans as one vast entity. However, the Perigondwanan shelf sections were isolated somewhat from this super-ocean by the Cimmerian Continent and Lhasa Block, which were spreading away from the Perigondwanan margin and opening up the Neotethyan Ocean (Fig. 1). This young, narrow ocean spanned a broad range of latitudes from the equator to greater than 60°S, with the result that circulation may have been driven by the climatic gradient along its length. For example, the generation of warm, saline waters in lower latitudes may have supplied a deep-ocean conveyor, such that deep waters were oxygenated in much the same way as the present-day Mediterranean. Whatever the circulation regime, the Cimmerian continent is likely to have isolated Neotethys from the oceanographic changes recorded in the sediments of Panthalassa and equatorial Paleotethys. This isolation enabled the region to avoid the end-Permian mass extinction, although it was only a temporary respite. The Permian benthic holdovers of the South Tibetan fauna succumbed in the late Griesbachian, coincident with the spread of oxygen-poor waters during a prolonged phase of deepening.

ACKNOWLEDGEMENTS

The Royal Society and the Chinese National Natural Science Foundation are thanked for funding fieldwork in Tibet. Yin Jiarun, Wang Xiaoqiao, and Tony Hallam are thanked for help with logistics in this country. Fieldwork in British Columbia was funded by NERC grant GR3/11966, and much logistical support was provided by John-Paul Zonneveld of the Geological Survey of Canada. Kiyoko Kuwahara is thanked for identifying the radiolaria of the Fantasque Formation.

REFERENCES

BASSOULLET, J.P., and COLCHEN, M., 1977, La limite Permien–Trias dans le domaine tibétien de l'Himalaya du Népal (Annapurnas-Ganesh Himal): Ecologie et Géologie de l'Himalaya: Colloques Internationaux du Centre National de la Recherche Scientifique, v. 268, p. 41–52.

BASSOULLET, J.P., and MOUTERDE, R., 1977, Les Formations sédimentaires Mesozoiques du domain tibetien de l'Himalaya du Nepal: Ecologie et Géologie de l'Himalaya: Colloques Internationaux du Centre National de la Recherche Scientifique, v. 268, p. 53–59.

BEAUCHAMP, B., 1994, Permian climatic cooling in the Canadian Arctic: *in* Klein, G.D., ed., Pangea: Paleoclimate, Tectonics and Sedimentation During Accretion, Zenith and Break-up of a Supercontinent: Geological Society of America Special Paper, v. 288, p. 229–246.

BEAUCHAMP, B., and BAUD, A., 2002, Growth and demise of Permian biogenic chert along northwest Pangea: evidence for end-Permian collapse of thermohaline circulation: Palaeogeography, Palaeoclimatology, Palaeoecology, v. 184, p. 37–64.

BOWRING, S.A., ERWIN, D.H, JIN Y.G., MARTIN, M.W., DAVIDEK, K., and WANG W., 1998, U/Pb zircon geochronology and tempo of the End-Permian mass extinction: Science, v. 280, p. 1039–1045.

BURNS, S.J., MCKENZIE, J.A., and VASCONCELOS, C., 2000, Dolomite formation and biogeochemical cycles in the Phanerozoic: Sedimentology, v. 47(suppl. 1), p. 49–61.

DAGYS, A., 1994, Correlation of the lowermost Triassic: Albertiana, v. 14, p. 38–44.

ERWIN, D.H., BOWRING, S.A., and JIN Y.-G., 2002, End-Permian mass extinctions: a review: *in* Koeberl, C., and MacLeod, K.G., eds., Catastrophic Events and Mass Extinctions: Impacts and Beyond: Geological Society of America Special Paper, v. 356, p. 363–383.

FAURE, G., 1986, Principles of Isotope Geology: John Wiley and Sons, New York, 630 p.

FLÜGEL, E., and REINHARDT, J., 1989, Uppermost Permian reefs in Skyros (Greece) and Sichuan (China): implications for the Late Permian extinction event: PALAIOS, v. 4, p. 502–518.

GARZANTI, E., 1999, Stratigraphy and sedimentary history of the Nepal Tethys Himalaya passive margin: Journal of Asian Earth Sciences, v. 17, p. 805–827.

GARZANTI, E., ANGIOLINI, L., and SCIUNNACH, D., 1996, The Permian Kuling Group (Spiti, Lahaul and Zanskar; N.W. Himalaya): sedimentary evolution during rift/drift transition and initial opening of Neotethys: Rivista Italiana Paleontologia Stratigrafia, v. 102, p. 175–200.

GARZANTI, E., NICORA, A., & RETTORI, R., 1998, Permo-Triassic boundary and Lower to Middle Triassic in South Tibet: Journal of Asian Earth Sciences, v. 16, p. 143–157.

HALLAM, A., and WIGNALL, P. B., 1997, Mass Extinctions and Their Aftermath: Oxford University Press, Oxford, 320 p.

HENDERSON, C. M., 1997, Uppermost Permian conodonts and the Permian–Triassic boundary in the Western Canadian Sedimentary Basin: Bulletin of Canadian Petroleum Geology, v. 45, p. 693–707.

HENDERSON, C. M., and MEI, S., 2000, Preliminary cool water Permian conodont zonation in North Pangea: a review: Permophiles, v. 36, p. 16–23.

HOLSER, W.T., SCHÖNLAUB, H.P., BOECKLEMANN, K., MAGARITZ, M., and ORTH, C.J., 1991, The Permian-Triassic of the Gartnerkofel-1 core (Carnic Alps, Austria): synthesis and conclusions: Abhandlungen der Geologischen Bundesanstalt, v. 45, p. 213–232.

HOTINSKI, R.M., BICE, K.L., KUMP, L.R., NAJJAR, R.G., and ARTHUR, M.A., 2001, Ocean stagnation and end-Permian anoxia: Geology, v. 29, p. 7–10.

ISOZAKI, Y., 1994, Superanoxia across the Permo-Triassic boundary: recorded in accreted deep-sea pelagic chert in Japan: Memoir of the Canadian Society of Petroleum Geology, v. 17, p. 805–812.

ISOZAKI, Y., 1997, Permo-Triassic boundary superanoxia and stratified superocean: records from lost deep sea: Science, v. 276, p. 235–238.

JIN, Y., SHEN, S.Z., ZHU, Z., MEI, S., and WANG, W., 1996, The Selong section, candidate of the global stratotype and section, and point of the Permian-Triassic boundary: *in* Yin H.-F., ed., The Palaeozoic-Mesozoic Boundary Candidates of Global Stratotype Section and Point of the Permian-Triassic Boundary: China University of Geosciences, Beijing, p. 127–137.

KOBAYASHI, F., 1999, Tethyan uppermost Permian (Dzhulfian and Dorashamian) foraminiferal faunas and their palaeogeographic and tectonic implications: Palaeogeography, Palaeoclimatology, Palaeoecology, v. 150, p. 279–308.

LIU, G., and EINSELE, G., 1994, Sedimentary history of the Tethyan basin in the Tibetan Himalayas: Geologisches Rundschau, v. 83, p. 32–61.

MEI, S.L., 1996, Restudy of conodonts from the Permian-Triassic boundary beds at Selong and Meishan and the natural Permian-Triassic boundary: *in* Wang, H.-Z., and Wang, X,-L., eds., Centennial Memorial Volume of Professor Sun Yunzhu: Palaeontology and Stratigraphy: China University of Geosciences Press, Wuhan, p. 141–148.

MOSLOW, T.F., and DAVIES, G.R., 1997, Turbidite reservoir facies in the Lower Triassic Montney Formation, west-central Alberta: Bulletin of Canadian Petroleum Geology, v. 45, p. 507–536.

MURCHEY, B.L., and JONES, D.L., 1992, A mid-Permian chert event: widespread deposition of biogenic siliceous sediments in coastal, island arc and oceanic basins: Palaeogeography, Palaeoclimatology, Palaeoecology, v. 96, p. 161–174.

MYERS, K.J., and WIGNALL, P.B., 1987, Understanding Jurassic organic-rich mudrocks—new concepts using gamma-ray spectrometry and palaeoecology: examples from the Kimmeridge Clay of Dorset and the Jet Rock of Yorkshire: *in* Leggett, J.K., and Zuffa, G.G., eds., Marine Clastic Sedimentology: Graham and Trotman, London, p. 172–189.

NAKAZAWA, K., KAPOOR, H.M., ISHII, K., BANDO, Y., OKIMURA, Y., and TOKUOKA, T., 1975, The Upper Permian and Lower Triassic in Kashmir, India: Memoir of the Faculty of Science, Kyoto University, Geology and Mineralogy Series, v. 42, p. 1–106.

OKIMURA, Y., ISHII, K., and ROSS, C.A., 1985, Biostratigraphical significance and faunal provinces of Tethyan Late Permian small Foraminifera: *in* Nakazawa, K., and Dickens, J.M., eds., The Tethys, Her Paleogeography and Paleobiogeography from Paleozoic to Mesozoic: Tokai University Press, Tokyo, p. 115–138.

ORCHARD, M.J., NASSICHUK, W.W., and RUI, L., 1994, Conodonts from the Lower Griesbachian *Otoceras latilobatum* Bed of Selong, Tibet and the position of the Permian-Triassic boundary: Memoir of the Canadian Society of Petroleum Geologists, v. 17, p. 823–843.

ORCHARD, M.J., and TOZER, E.T., 1997, Triassic conodont biochronology, its calibration with the ammonoid standard, and a biostratigraphic summary for the Western Canadian Sedimentary Basin: Bulletin of Canadian Petroleum Geology, v. 45, p. 675–692.

PAKISTANI-JAPANESE RESEARCH GROUP, 1985, Permian and Triassic systems in the Salt Range and Surghar Range, Pakistan: *in* Nakazawa, K., and Dickins, J.M., eds., The Tethys: Her Paleogeography and Paleobiogeography from Paleozoic to Mesozoic: Tokai University Press, Tokyo, p. 221–312.

RETALLACK, G.J., 1999, Postapocalyptic greenhouse paleoclimate revealed by earliest Triassic paleosols in the Sydney Basin, Australia: Bulletin of the Geological Society of America, v. 111, p. 52–70.

ROUCHY, J.M., and MONTY, C., 2000, Gypsum microbial sediments: Neogene and modern examples: *in* Riding, R.E., and Amramik, S.M., eds., Microbial Sediments: Springer-Verlag, Berlin, p. 209–216.

SANO, H., and NAKASHIMA, K., 1997, Lowermost Triassic (Griesbachian) micrbial bindstone-cementstone facies, southwest Japan: Facies, v. 36, p. 1–24.

SASHIDA, K., IGO, H., ADACHI, S., UENO, K., KAJIWARA, Y., NAKORNSRI, N., and SADSUD, A., 2000, Late Permian to Middle Triassic radiolarian faunas from northern Thailand: Journal of Paleontology, v. 74, p. 789–811.

SCOTESE, C.R., and LANGFORD, R.P., 1995. Pangea and the paleogeography of the Permian: *in* Scholle, P.A., Peryt, T.M., and Ulmer-Scholle, D.S., eds., The Permian of Northern Pangea 1: Springer-Verlag, Berlin, p. 3–19.

SHEN, S.-Z., ARCHBOLD, N.W., and SHI G.-R., 2001, A Lopingian (Late Permian) brachiopod fauna from the Qubuerga Formation at Shengmi in the Mount Qomolongma region of southern Xizang (Tibet), China: Journal of Paleontology, v. 75, p. 274–283.

SHEN, S.Z., ARCHBOLD, N.W., SHI G.R., and CHEN, Z.Q., 2000, Permian brachiopods from the Selong Xishan section, Xizang (Tibet), China. Part 1: Stratigraphy, Strophomenida, Productida and Rhynchonellida: Geobios, v. 33, p. 725–752.

SHEN, S.Z., and JIN, Y., 1999, Brachiopods from the Permian-Triassic boundary beds at the Selong Xishan section, Xizang (Tibet), China: Journal of Asian Earth Sciences, v. 17, p. 547–559.

SHUKLA, A.D., BHANDARI, N., and SHUKLA, P.N., 2002, Chemical signatures of the Permian-Triassic transitional environment in Spiti Valley, India: *in* Koeberl, C., and MacLeod, K.G., eds., Catastrophic Events and Mass Extinctions: Impacts and Beyond: Geological Society of America Special Paper, v. 356, p. 363–383.

STAMPFLI, G., MARCOUX, J., and BAUD, A., 1991, Tethyan margins in space and time: Palaeogeography, Palaeoclimatology, Palaeoecology, v. 87, p. 373–409.

TWITCHETT, R.J., LOOY, C.V., MORANTE, R., VISSCHER, H., and WIGNALL, P.B., 2001, Rapid and synchronous collapse of marine and terrestrial ecosystems during the end-Permian biotic crisis: Geology, v. 29, p. 445–454.

TWITCHETT, R.J., and WIGNALL, P.B., 1996, Trace fossils and the af-

termath of the end-Permian mass extinction: Palaeogeography Palaeoclimatology Palaeoecology, v. 124, p. 137–151.

WANG, K., GELDSETZER, H.H.J., and KROUSE, H.R., 1994, Permian-Triassic extinction: organic $d^{13}C$ evidence from British Columbia, Canada: Geology, v. 22, p. 580–584.

WANG, Y., CHEN, C., RUI, L., WANG, Z., LIAO, Z., and HE, J., 1989, A potential global stratotype of Permian-Triassic boundary: Developments in Geoscience: (Contribution to 28th International Geological Congress, 1989, Washington D.C.): Science Press, Beijing, p. 221–229.

WATERHOUSE, J.B., 1977, The Permian rocks and faunas of Dolpo, north-west Nepal: Ecologie et Géologie de l'Himalaya: Colloques Internationaux du Centre National de la Recherche Scientifique, v. 268, p. 481–496.

WIGNALL, P.B., 1994, Black Shales: Oxford University Press, Oxford, 130 p.

WIGNALL, P.B., and HALLAM, A., 1992, Anoxia as a cause of the Permian/Triassic extinction: facies evidence from northern Italy and the western United States: Palaeogeography, Palaeoclimatology, Palaeoecology, v. 93, p. 21–46.

WIGNALL, P. B., and HALLAM, A., 1993, Griesbachian (earliest Triassic) palaeoenvironmental changes in the Salt Range, Pakistan and southwest China and their bearing on the Permo-Triassic mass extinction: Palaeogeography, Palaeoclimatology, Palaeoecology, v. 102, p. 215–237.

WIGNALL, P.B., and HALLAM, A., 1996, Facies change and the end-Permian mass extinction in S.E. Sichuan, China: PALAIOS, v. 11, p. 587–596.

WIGNALL, P.B., KOZUR, H., and HALLAM, A., 1996, The timing of palaeoenvironmental changes at the Permian/Triassic (P/Tr) boundary using conodont biostratigraphy: Historical Biology, v. 12, p. 39–62.

WIGNALL, P.B., MORANTE, R., and NEWTON, R., 1998, The Permo–Triassic transition in Spitsbergen: $\delta^{13}C_{org}$ chemostratigraphy, Fe and S geochemistry, facies, fauna and trace fossils: Geological Magazine, v. 135, p. 47–62.

WIGNALL, P.B., and NEWTON, R., 1998, Pyrite framboid diameter as a measure of oxygen deficiency in ancient mudrocks: American Journal of Science, v. 298, p. 537–552.

WIGNALL, P.B., and TWITCHETT, R.J., 1996, Oceanic anoxia and the end Permian mass extinction: Science, v. 272, p. 1155–1158.

WIGNALL, P.B., and TWITCHETT, R.J., 2002, Extent, duration and nature of the Permian–Triassic superanoxic event: *in* Koeberl, C., and MacLeod, K.G., eds., Catastrophic Events and Mass extinctions: Impacts and Beyond: Geological Society of America Special Paper, v. 356, p. 395–413.

WILKIN, R.T., ARTHUR, M.A., and DEAN, W.E., 1997, History of water-column anoxia in the Black Sea indicated by pyrite framboid size distributions: Earth and Planetary Science Letters, v. 148, p. 517–525.

WILKIN, R.T., BARNES, H.L., and BRANTLEY, S.L., 1996, The size distribution of framboidal pyrite in modern sediments: An indicator of redox conditions: Geochimica et Cosmochimica Acta, v. 60, p. 3897–3912.

WOODS, A.D., and BOTTJER, D.J., 2000, Distribution of ammonoids in the Lower Triassic Union Wash Formation (Eastern California): evidence for paleoceanographic conditions during the recovery from the end-Permian mass extinction: PALAIOS, v. 15, p. 535–545.

WOODS, A.D., BOTTJER, D.J., MUTTI, M., and MORRISON, J., 1999, Lower Triassic large sea-floor carbonate cements: their origin and a mechanism for the prolonged biotic recovery from the end-Permian mass extinction: Geology, v. 27, p. 645–648.

YAO, A., and KUWAHARA, K., 1997, Radiolarian faunal change from Late Permian to Middle Triassic times: News of Osaka Micropaleontologists Special Volume, v. 10, p. 87.

YIN, H.F., 1993, Candidates for Global Stratotype Sections of the Permian-Triassic boundary: Albertiana, v. 12, p. 45–48.

ACCEPTED OCTOBER 1, 2002